

Optimizing Cost through Dynamic Stochastic Resetting

Deepak Gupta^{1,2,*} and Bart Cleuren^{1,†}

¹*UHasselt, Faculty of Sciences, Theory Lab, Agoralaan, 3590 Diepenbeek, Belgium*

²*Department of Physics, Indian Institute of Technology Indore,
Khandwa Road, Simrol, Indore-453552, India*

The cost of stochastic resetting is considered within the context of a discrete random walk model. In addition to standard stochastic resetting, for which a reset occurs with a certain probability after *each* step, we introduce a novel resetting protocol which we dubbed *dynamic resetting*. This protocol entails an additional dynamic constraint related to the direction of successive steps of the random walker. We study this novel protocol for a one-dimensional random walker on an infinite lattice. We analyze the impact of the constraint on the walker's mean-first passage time and the cost (fluctuations) of the resets as a function of distance of target from the resetting location. Further, cost optimized search strategies are discussed.

I. INTRODUCTION

Unraveling efficient search protocols is an attractive field of research in various scientific disciplines [1, 2] ranging from biology [3], chemistry [4], to ecology [5]. Animals foraging for food [6, 7], *E. coli* diffusing towards higher food concentration [8], and transcription factor finding DNA promoter sites [9, 10] are some of the examples of search mechanisms displayed by biological organisms. In computer science, researchers design efficient search algorithms to solve hard combinatorial problems [11, 12]. Recent research discovered that sudden restart of a search process can dramatically change the diffusive searcher's mean first passage time to find the target [13]. In contrast, this mean first passage time of an unbiased random walker in the absence of restart protocol diverges. The common intuition behind how the restart mechanism expedites the search process is by truncating those trajectories that move further away from the target, and which would have contributed to longer search times. See Ref. [14] and references therein for a detailed review of this topic.

The traditional stochastic resetting (tSR) mechanism is implemented by restarting/resetting the underlying (inherent) dynamical process at random time intervals [13]. Thus, tSR is an intermittent dynamical process whereby the overall mechanism involves slow excursions due to the inherent system's dynamics followed by sudden/instantaneous restarts. Several variants of tSR have been explored in the past, notably including the space- [15] and time-dependent resetting [16, 17], power-law resetting [18], resetting in discrete-space and discrete-time models [19], asymmetric resetting [20], and refractory period resetting [21–23]. Several applications of stochastic resetting have been demonstrated for a wide variety of processes, such as the Mpemba effect [24, 25], molecular dynamics simulations [26], overfitting protocols [27], speed-limit [28], fast equilibration techniques [29], erasure [30], Maxwell's demon [31], and income dynamics [32, 33].

In contrast to the tSR protocol, in this paper, we introduce a novel *dynamic stochastic resetting* (dSR) protocol. This protocol is inspired by, and related to, a resetting mechanism previously considered in the context of Brownian Donkeys [34]. These donkeys are a type of Brownian motors with absolute negative mobility, meaning the peculiar property that the motor on average moves against an externally applied bias (see for example [35–39] for other representative examples). In the dSR protocol, a random walker (depicting the underlying dynamical process) is allowed to reset (to a predetermined location) only when the *number of consecutive steps in the same direction* (later defined as σ) reaches a threshold

* phydeepak.gupta@gmail.com

† bart.cleuren@uhasselt.be

value N_r . The threshold value N_r hence represents the minimal number of consecutive steps in the same direction before a reset can occur. Upon a change in direction or a reset, the value of σ is re-initialised. In the limit of $N_r = 1$, both frameworks (dSR and tSR) are identical. We stress that dSR is different than the space-dependent resetting framework [15, 20], where in the latter the resetting occurs when the process crosses a threshold value.

In this paper, we apply the dSR protocol on a random walker on a one-dimensional infinite lattice. Herein, we compute the mean first passage time (MFPT) and its standard deviation, and the coefficient of variation, each as a function of the threshold value N_r and the target location. Then, we extend our analysis to estimate the cost of dynamical stochastic resetting for an ensemble of the first passage trajectories. We highlight that thermodynamic cost of stochastic resetting has been previously investigated for different settings including instantaneous resetting [40, 41], proportional [42] and stochastic return [43, 44], first passage process [45, 46], unidirectional process [47, 48], uncertainty relations [49], and intermittent switching potentials [29, 30].

We investigate the impact of dSR on the first passage time and the cost of resetting and compare these results with tSR. We motivate ourselves from the perspective of computer search algorithms, where one requires time-efficient protocols to solve hard combinatorial problems [11, 12]. tSR is an interesting route to reduce effective computational time [50]. However, one of the shortcomings of tSR is that the MFPT diverges for stronger resetting (in the limit of resetting's frequency going to infinity). On the contrary, we will show that dSR reduces the MFPT (in comparison to tSR) in this particular limit. We also discuss the cost-effectiveness of dSR's search protocols. To the best of our knowledge, such a dynamic resetting protocol was not investigated earlier, which also motivates us to study herein.

This paper is organized as follows. Section II describes the algorithm of the dynamical stochastic resetting protocol for a one-dimensional random walk. Section III discusses the statistics of the first passage time and the mean cost of dynamic resetting. We summarize our paper in Sec. IV. The stationary probability distribution of random walker for tSR is discussed in Appendix A. The calculations for the moment generating functions of the first passage time and cost for tSR are, respectively, relegated to Appendices B1 and B2. We discuss the mean first passage time in the limit of the resetting probability $p_r \rightarrow 1$ in Appendix C. Appendix D presents a comparison of the mean first passage time obtained using the window resetting (discrete analogy of Ref. [15]) with that of dSR. We discuss the mean cost for the case when the threshold distance is larger than the target distance in Appendix E. Method of dSR simulations is discussed in Appendix F.

II. SETUP

We consider a random walker (RW) on a one-dimensional (1D) infinite lattice. The spatial position is labeled by $x \in \mathbb{Z}$. In the context of resetting, the RW starts at an initial position x_0 and moves about until it hits the target at position x_T . Additionally, we define x_r as the spatial position towards the RW is relocated upon a resetting event. Jumps to the right (left) occur with probability p (q) such that $p + q = 1$. Hence, both space and time are discrete. For the resetting mechanism we introduce an additional counter σ which keeps track of the length of the last sequence of successive steps taken by the RW *in the same direction*. This counter can be 0 (at the initial condition and also immediately after a reset occurs) or positive/negative if the last step was to the right/left. A step in the same direction as the previous one will increase (for consecutive steps to the right) the counter by +1, and decrease the (negative) counter by -1 for consecutive steps to the left. A change in direction of the RW sets the counter to +1 (-1) if previous steps were to the left (right) followed by a step to the right (left). In the dynamical protocol a reset is only allowed, with a certain probability p_r , when this counter is greater or equal to a threshold value, that is when $|\sigma| \geq N_r$. Hence, as stated before, this parameter N_r represents the minimal number of consecutive steps in the same direction before a reset can occur. Clearly, when $N_r = 1$ we recover standard stochastic resetting tSR.

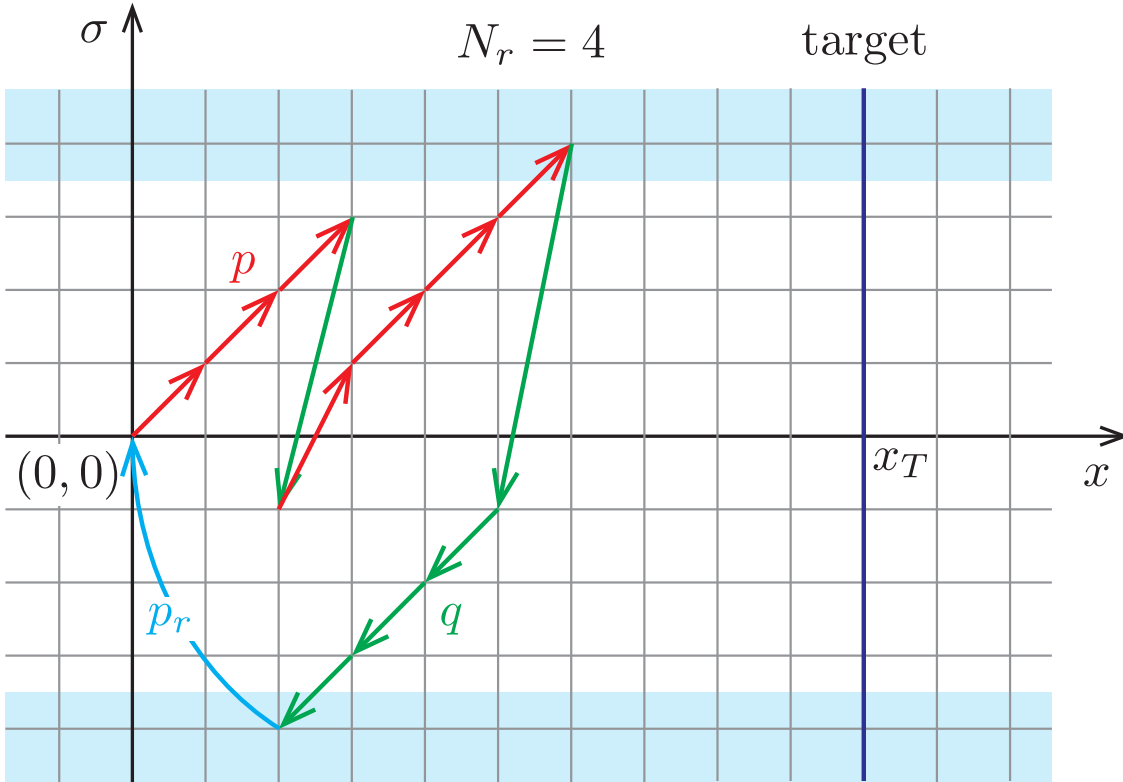


FIG. 1. Sketch of a trajectory, starting at location $(0, 0)$, made by a random walker (RW) on a 1D infinite lattice $x \in \mathbb{Z}$, where x denotes the RW's position. The counter, σ , counts the number of steps made by RW in one direction. Hops to the right (left) occur with probability p ($q = 1 - p$). Resets to the resetting location $x = 0$ occur with a probability p_r whenever $|\sigma| \geq N_r$ (indicated by the blue regions). The counter, σ , is set to -1 ($+1$) when the RW switches its spatial direction from positive to negative (negative to positive). The solid blue line, at position x_T marks the position of the target: if the RW is on any point along this line after a complete move is made, the target is found and the movement stops.

It is clear that x alone is no longer a Markovian variable, and one needs to consider both x and σ in order to describe the full dynamics. As the RW moves about, a trajectory in the (x, σ) -plane is traced out. An example is given in Fig. 1: a RW starts at the origin $(0, 0)$ and explores the space until a reset occurs at position $(2, -4)$ after which the RW ends up back in the origin $(0, 0)$. As previously described, and as is made evident by the figure, as long as the RW moves in *the same* direction, the counter σ is increased (for a spatial jump to the right) or decreased (for a spatial jump to the left) by 1. A *change of direction* sets the counter to either $+1$ when the last jump was to the right and the jump(s) before the last one to the left, or -1 in the opposite case. A *complete move* or *time step* in the (x, σ) -plane involves two steps: first a spatial jump is made, as in the classical random walk setting. As a result of this jump both x and σ are updated. As a second step, given the updated value of σ , a check is made to determine whether σ reaches the threshold, that is whether $N_r \leq |\sigma|$. If this is the case, with probability p_r a reset is done. So both steps (first the spatial jump, then the check for a reset) comprises one complete move in the (x, σ) -plane. This is repeated until, after a complete move is done, the RW has reached the target located at a given position x_T . Note that the complete move implies that even if the RW is at x_T immediately after the spatial jump, one still has to check

for a reset (which can bring the RW back to the origin). If a reset occurs, the target in fact is not yet reached. The diagram below gives all possible moves, starting from the current state (x, σ) , together with the probability of the move and the conditions on σ :

$$(x, \sigma) \rightarrow \begin{cases} (x+1, \sigma+1) & \text{with probability } p \text{ for } 0 \leq \sigma < N_r - 1 \\ (x+1, \sigma+1) & \text{with probability } p(1-p_r) \text{ for } N_r - 1 \leq \sigma \\ (0, 0) & \text{with probability } pp_r \text{ for } N_r - 1 \leq \sigma \\ (x-1, \sigma-1) & \text{with probability } q \text{ for } -N_r + 1 < \sigma \leq 0 \\ (x-1, \sigma-1) & \text{with probability } q(1-p_r) \text{ for } \sigma \leq -N_r + 1 \\ (0, 0) & \text{with probability } qp_r \text{ for } \sigma \leq -N_r + 1 \\ (x+1, 1) & \text{with probability } p \text{ for } \sigma < 0 \\ (x-1, -1) & \text{with probability } q \text{ for } \sigma > 0, \end{cases} \quad (1)$$

In the absence of a target, the position distribution of the RW will reach a non equilibrium stationary state. Figure 2 shows the comparison between the stationary distributions (numerical simulation data) obtained for different threshold values N_r . We also show the comparison between analytical prediction (A12) for $N_r = 1$ with the numerical simulation data. As is intuitively clear, the distribution becomes wider as N_r increases. This is expected as the likelihood for a reset decreases for increasing N_r .

In this paper, our first objective is to study the statistics of the first passage time for different values of threshold distance N_r , as a function of target's distance, x_T , from RW's resetting location. The first passage time is the time taken by the RW starting from $x(0)$ and hitting the target at x_T for the first time:

$$n_{\text{FP}} \equiv \inf\{n; x(n) = x_T | x(0)\} . \quad (2)$$

The second quantity of the interest is the cost [45] of resetting until the random walker hits the target x_T for the first time:

$$C_\beta \equiv c \sum_{i=1}^{\mathcal{N}(n_{\text{FP}})} |x(i) - x_r|^\beta , \quad (3)$$

where c is the intrinsic cost associated with each resetting. $x(i)$ and x_r , respectively, are RW's position before and after the i -th resetting, β is an exponent, and $\mathcal{N}(n_{\text{FP}})$ is the number of reset events occurred before the system hitting the target for the first time. For convenience, we rescale C_β by c , such that the former becomes a dimensionless quantity:

$$C_\beta = \sum_{i=1}^{\mathcal{N}(n_{\text{FP}})} |x(i) - x_r|^\beta . \quad (4)$$

Both first passage time n_{FP} (2) and cost of reset C_β (4) are stochastic quantities. And while analytical computation of their statistics is untractable for $N_r > 1$, for the case $N_r = 1$ one can compute analytically the exact moment generating function of first passage time and the cost C_β . These are respectively given below (see Appendices B1 and B2 for detailed calculations):

$$\tilde{F}(z|x_0) = \frac{\tilde{F}_{\text{NR}}(z(1-p_r)|x_0)}{1 - zp_r\tilde{S}_{\text{NR}}(z(1-p_r)|x_0)} , \quad (5)$$

$$\tilde{\Phi}(k, 1|x_0) = \frac{\tilde{F}_{\text{NR}}(1-p_r|x_0)}{1 - p_r\tilde{\phi}_{\text{NR}}(k, 1-p_r|x_0)} . \quad (6)$$

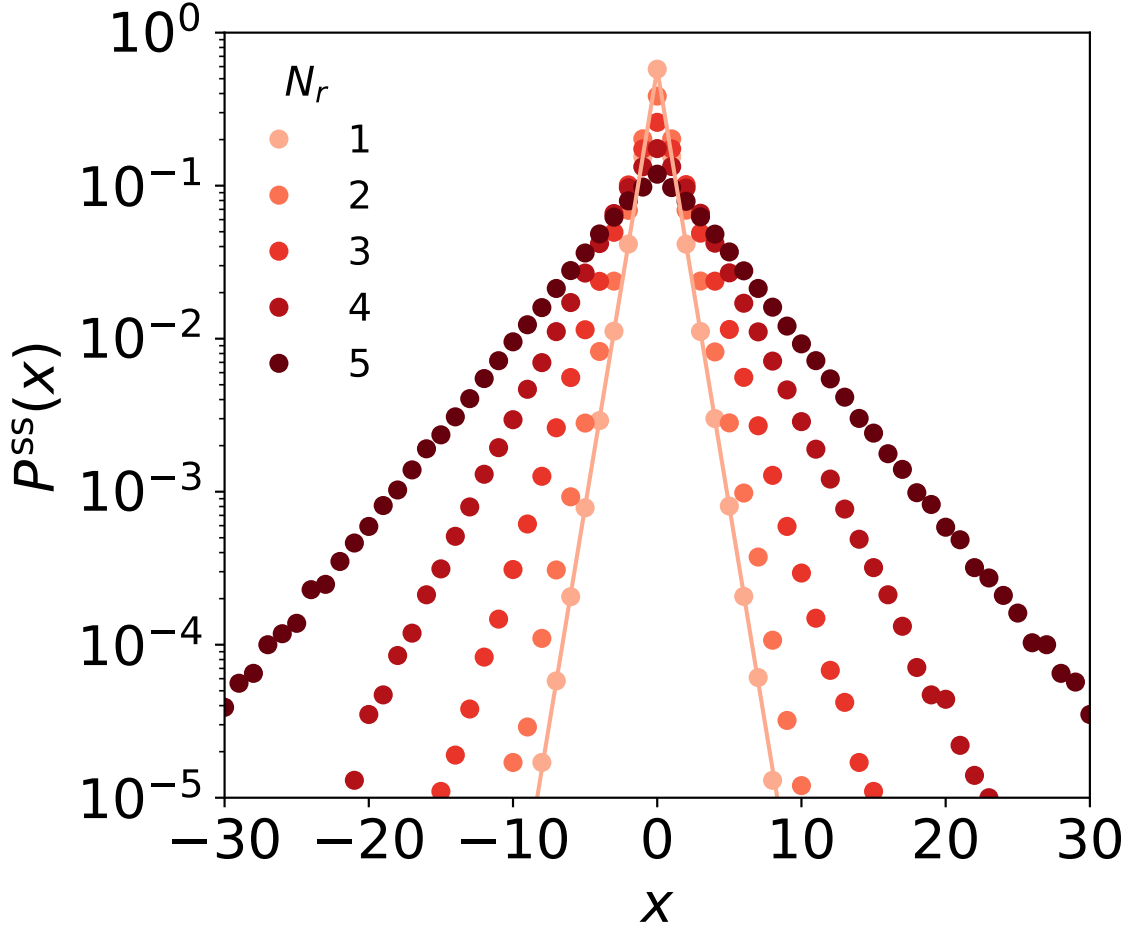


FIG. 2. Unbiased random walk ($p = q = 1/2$). Stationary probability distribution $P^{SS}(x)$ as a function of position x . Color intensity increases with N_r . Resetting probability $p_r = 0.5$. Solid line: Analytical prediction for $N_r = 1$ (A12). Time steps: 10^3 . Number of realizations: 10^6 .

For simplicity, here and in what follows, we consider the initial location x_0 and resetting location x_r to be the same, i.e., $x_r = x_0$. The quantities $\tilde{S}_{\text{NR}}(z|x_0)$ and $\tilde{F}_{\text{NR}}(z|x_0)$, respectively, are the z -transformed [?] survival probability and first passage distribution of the non-reset (NR) random walker starting from $x = x_0$ in the presence of an absorbing boundary at $x = x_T$. $\tilde{\phi}_{\text{NR}}(k, z|x_0)$ is the z -transformed reset-free moment generating function of the cost, averaged over ensemble of trajectories in the presence of absorbing boundary at x_T :

$$\tilde{\phi}_{\text{NR}}(k, z|x_0) \equiv \sum_{x=-\infty}^{x_T} e^{ik|x-x_0|^\beta} \tilde{P}_{\text{NR}}^{\text{abs}}(x, z|x_0). \quad (7)$$

Here, $\tilde{P}_{\text{NR}}^{\text{abs}}(x, z|x_0)$ is the z -transformed probability distribution function of random walker's positions, starting from $x = x_0$ and in the presence of absorbing boundary at $x = x_T$. Using Eqs. (5) and (6), we can compute the moments of first passage time and cost, and these are shown in Appendices B1 and B2.

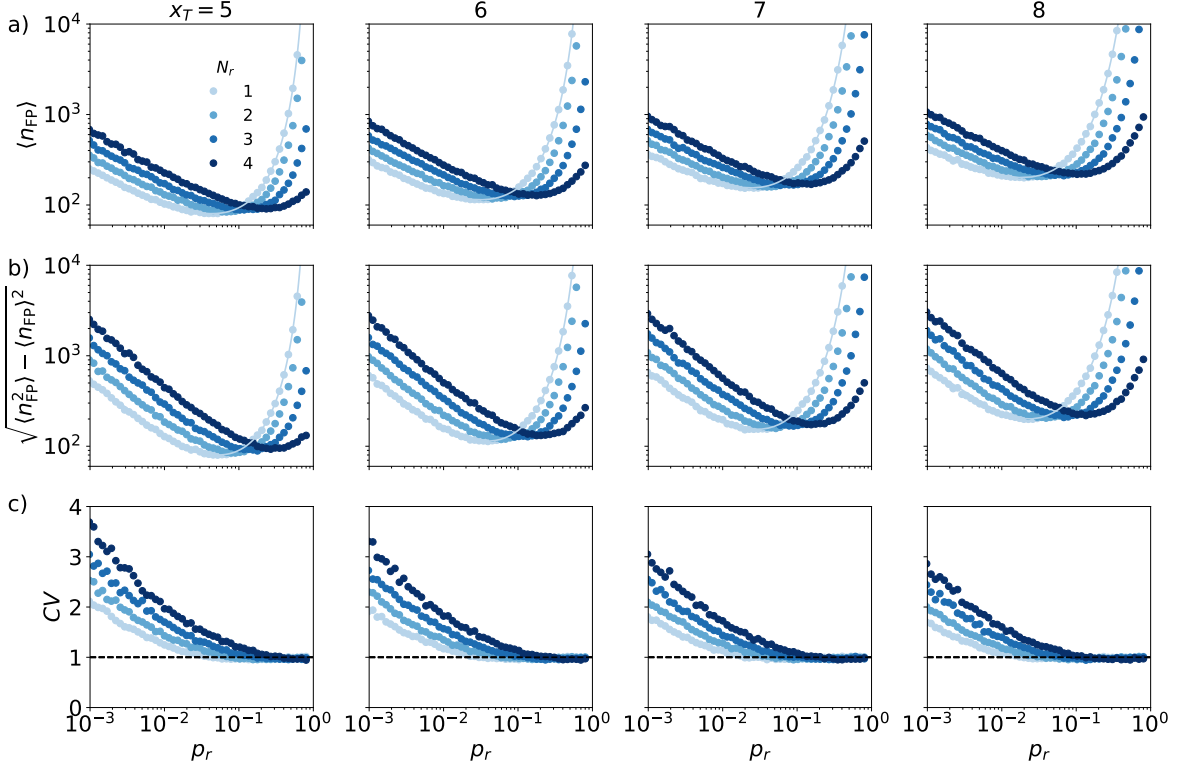


FIG. 3. Unbiased random walk ($p = q = 1/2$). (a) Mean first passage time $\langle n_{\text{FP}} \rangle$, (b) standard deviation $\sqrt{\langle n_{\text{FP}}^2 \rangle - \langle n_{\text{FP}} \rangle^2}$, and (c) coefficient of variation $CV \equiv \frac{\sqrt{\langle n_{\text{FP}}^2 \rangle - \langle n_{\text{FP}} \rangle^2}}{\langle n_{\text{FP}} \rangle}$, each as a function of reset probability p_r . x_T : Target's distance from the resetting location. The color intensity increases with the threshold distance N_r . (a-b) Solid curves are the analytical predictions [Eqs. (B23) and (B27)] for $N_r = 1$. (c) Horizontal dashed line corresponds to $CV = 1$. For all plots, resetting x_r and initial location x_0 are same (i.e., $x_r = x_0$) and number of realizations 10^4 .

For threshold distances $N_r > 1$ we compute the first passage time and cost using dSR discussed in Eq. (1) by using the numerical computations (see Appendix F for the methods of simulations).

III. RESULTS

In what follows we focus, for simplicity, on the symmetric random walk $p = q = 1/2$. First, we discuss the statistics of the first passage time, and then, show the results for the mean cost of resetting.

In the following, we discuss the first passage time for the case when the threshold distance is smaller than the target distance from the resetting location, i.e., $1 \leq N_r < x_T$. Figure 3a discusses the mean first passage time (MFPT), $\langle n_{\text{FP}} \rangle$, as a function of the resetting probability p_r for different threshold N_r and target distances x_T . Moreover, for $N_r = 1$, we show the comparison of numerical simulation result with the analytical result (B23). For each case, the MFPT diverges in the limit $p_r \rightarrow 0$. This is to be expected, as this limit corresponds to a reset-free random walk for which the MFPT diverges. In the opposite limit ($p_r \rightarrow 1$), the MFPT diverges for $N_r = 1$ and 2, respectively, for all $|x_T| > 0$ and $|x_T| > 1$ (Fig. C1). This is because for $N_r = 1$ the walker (starting from origin) forever stays at the

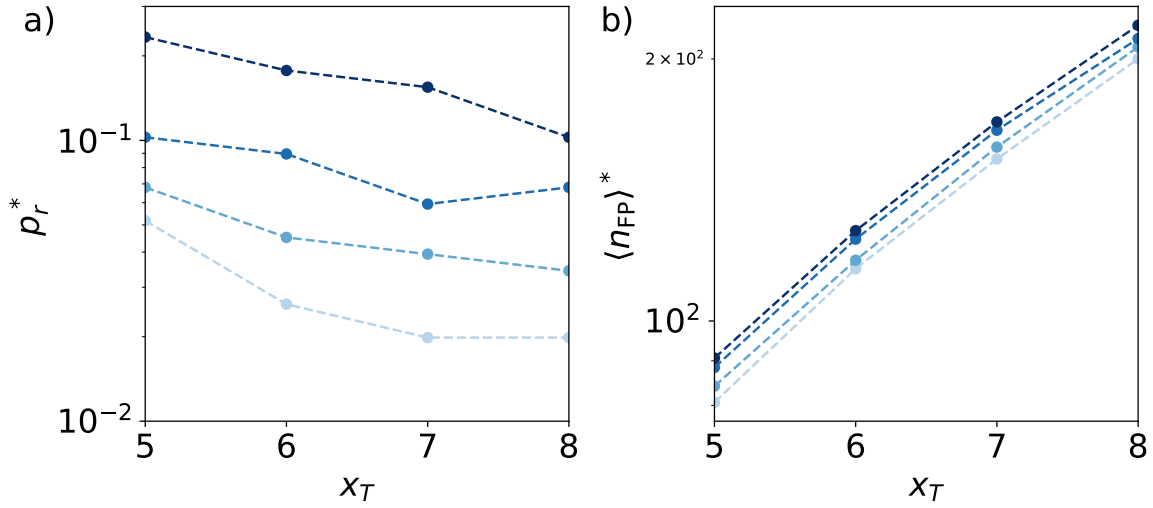


FIG. 4. Unbiased random walk ($p = q = 1/2$). (a) Optimal resetting probability p_r^* and (b) optimal mean first passage time $\langle n_{\text{FP}} \rangle^*$, each as a function of target's distance from the resetting location x_T . The color intensity increases with threshold distance N_r (Fig. 3). Connecting lines are guide to the eye.

origin (i.e., the resetting location), and for $N_r = 2$ the walker only explores the lattice points $-1, 0, 1$. For larger $N_r > 2$ the MFPT is finite for $p_r = 1$ (Fig. C1). It is clear from Figure 3a that the MFPT has a global minimum for each N_r . For a fixed $p_r \ll p_r^*(N_r = 1)$, the MFPT increases with N_r , where

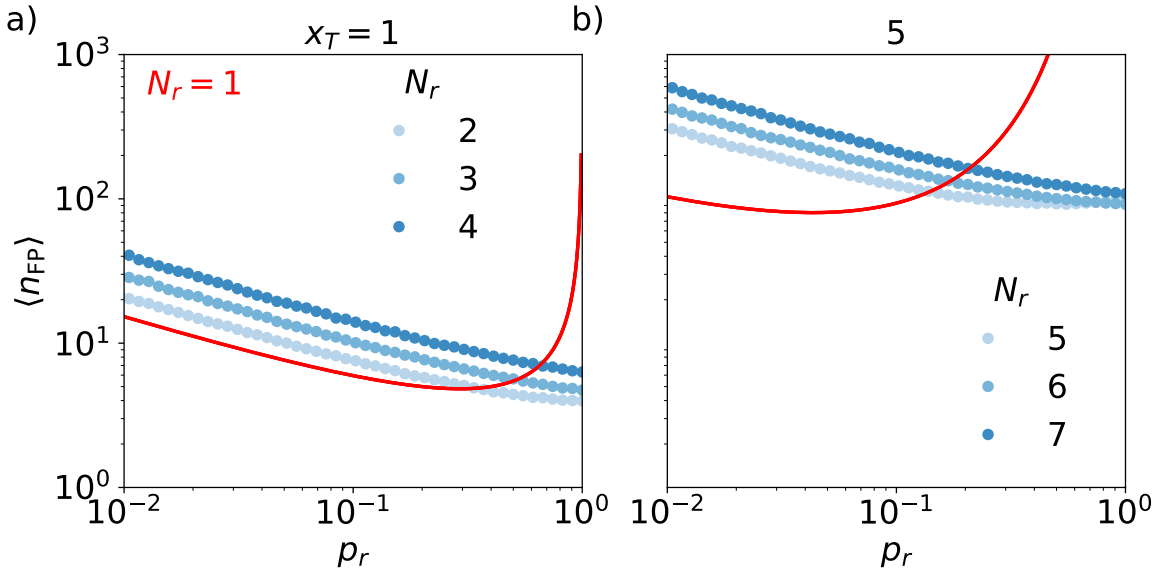


FIG. 5. Unbiased random walk ($p = q = 1/2$). Mean first passage time, $\langle n_{\text{FP}} \rangle$, as a function of resetting probability p_r . Symbols: Numerical simulation data. Red curve: Analytical result for $N_r = 1$. Blue: a) $x_T = 1$ and $N_r = 2, 3, 4$, and b) $x_T = 5$ and $N_r = 5, 6, 7$.

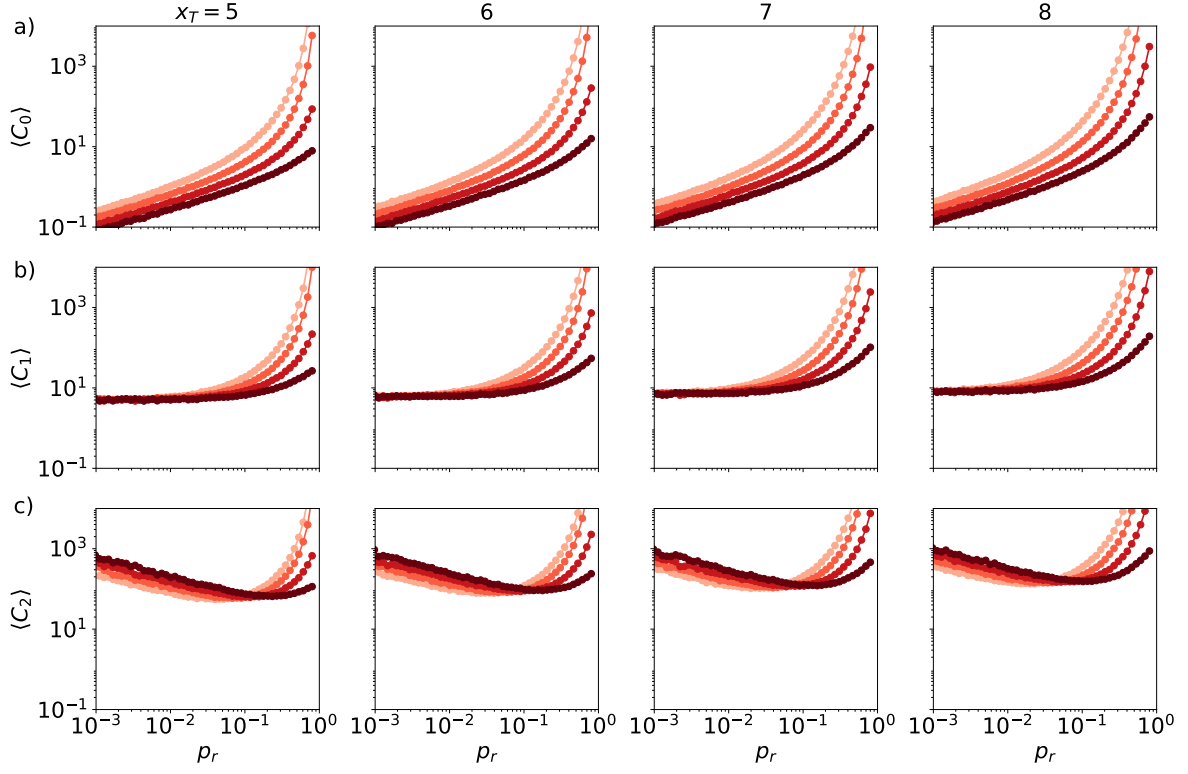


FIG. 6. Unbiased random walk ($p = q = 1/2$). Mean cost (4) as a function of reset probability p_r . The color intensity increases with threshold distance N_r (Fig. 3). Connecting lines are guide to the eye.

$p_r^*(N_r)$ is the optimal resetting probability for N_r :

$$p_r^*(N_r) \equiv \operatorname{argmin}_{p_r \in [0,1]} \langle n_{\text{FP}} \rangle. \quad (8)$$

This is because the dynamical resetting protocol reduces the probability of a reset as compared to the standard resetting protocol with $N_r = 1$. Hence, the MFPT increases by those trajectories which wander off in the opposite direction of the target. On the other hand, for $p_r \gg p_r^*(N_r = 1)$, a larger N_r allows the RW to explore more space before a reset occurs. And this helps the random walker to find the target. Increase in the target's distance increases the MFPT for each fixed N_r , as expected. Standard deviation (Fig. 3b) of the first passage time also displays similar behavior. Figure 3c shows the coefficient of variation $CV \equiv \frac{\sqrt{\langle n_{\text{FP}}^2 \rangle - \langle n_{\text{FP}} \rangle^2}}{\langle n_{\text{FP}} \rangle}$ as a function of p_r . In the limit $p_r \rightarrow 0$, the order of fluctuation relative to mean goes higher for higher threshold distance N_r ; this implies the first passage distribution becomes wider as N_r increases. Surprisingly, for larger resetting probability, $CV \approx 1$ for all cases.

Figure 4a discusses the variation of the optimal resetting probability p_r^* (8) as a function of the target's distance, x_T . For each N_r , p_r^* decays as x_T increases. This is expected because one has to reduce the resetting probability so that the random walker could explore more space in order to hit the target placed far away. Eventually, this increases the optimal MFPT $\langle n_{\text{FP}} \rangle_{p_r \rightarrow p_r^*}$ (Fig. 4b). Moreover, Fig. 4b shows that MFPT has a global minimum with respect to N_r at $N_r = 1$.

Figure 5 discusses the case for $N_r \geq x_T$, and it shows that for $N_r > x_T$, optimal MFPT is achieved for $p_r \rightarrow 1$. This is because dSR resets a *specific* fraction of trajectories which perform directed

random walk in consecutive steps until it hits the threshold N_r , other fraction of trajectories will hit the absorbing boundary without experiencing resetting. (This is in contrary to tSR where each trajectory can be reset with probability p_r .) Moreover, the probability of resetting these trajectories increases with p_r ; therefore, the mean first passage time decreases monotonically. For each fixed target location, MFPT is optimized with respect to N_r , and its optimal value is $N_r^* = x_T + 1$ (see also Fig. C1 for $p_r = 1$). Additionally, for $N_r \rightarrow \infty$, MFPT is expected to diverge for all p_r , since this limit corresponds to a reset-free random walker. Finally, in Fig. D1 and Appendix D, we discuss a comparison of the mean first passage time between the dynamic and window stochastic resetting (in analogy with Ref. [15]). It shows that dynamic stochastic resetting is better in the limit $p_r \rightarrow 1$ when $N_r < x_T$; otherwise, for $N_r > x_T$ window resetting has lower mean first passage time for all p_r .

Next we turn our attention towards the cost of resetting C_β for $N_r < x_T$. Figure 6 shows mean cost of resetting, $\langle C_\beta \rangle$ (4), as a function of resetting probability, p_r , for different threshold N_r and target distances, x_T . (See Fig. B1 for the comparison between analytical and numerical simulation results for $N_r = 1$.) In each panel of Fig. 6a, the mean constant cost $\langle C_0 \rangle$ (or the mean number of resets) increases monotonically. This is expected since increasing p_r , number of resets also increases. For each fixed p_r , $\langle C_0 \rangle$ reduces as N_r increases. This is because increasing N_r reduces the probability of resetting. $\langle C_0 \rangle$ increases as x_T increases, as expected. Linear cost $\langle C_1 \rangle$ also increases with p_r (Fig. 6b), whereas the quadratic cost $\langle C_2 \rangle$ shows non-monotonic behavior. In the limit $p_r \rightarrow 0$, $\langle C_{1,2} \rangle \neq 0$. This is because herein whenever the reset happens, the walker returns from very far distance, this gives non-zero value of the mean cost [44, 45]. The behavior of the mean cost strongly depends on the exponent β (4). Additionally, we find for $N_r \geq x_T$ results are qualitatively similar (Fig. E1).

Figure 7 shows the ratio of mean of constant cost $\langle C_\beta \rangle$ to MFPT as a function of resetting probability p_r . In each panel, for each N_r , the data is plotted for two target's distances $x_T = 5, 8$. Figure 7(a-d) shows this ratio is independent of target distance, whereas we observe weak dependence on target

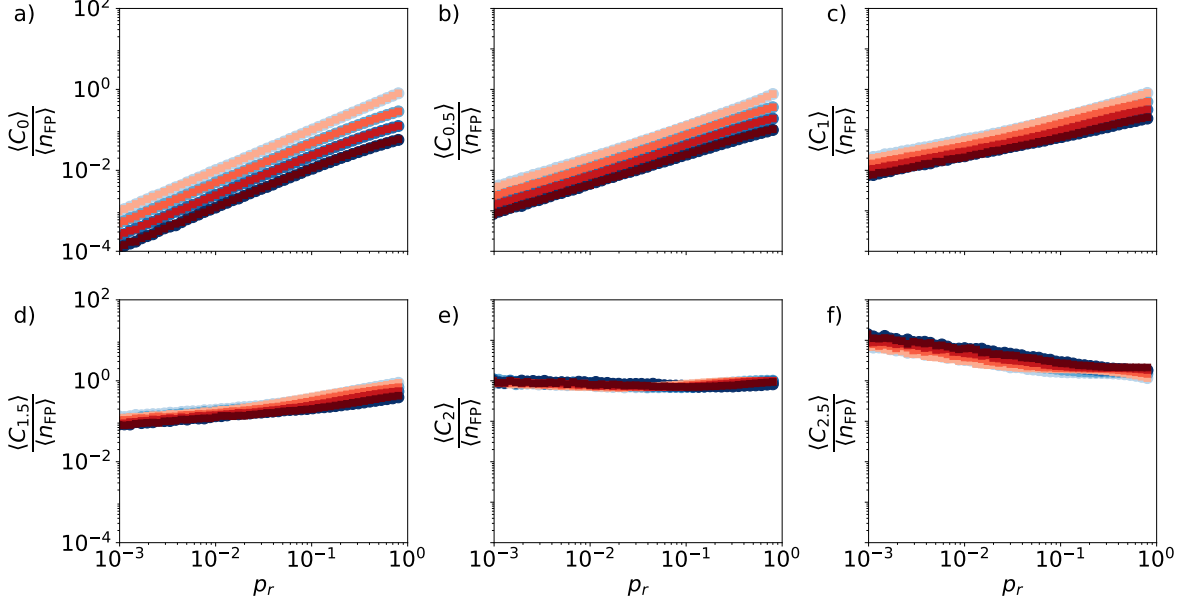


FIG. 7. Unbiased random walk ($p = q = 1/2$). Ratio of average cost, $\langle C_\beta \rangle$ (4) to the mean first passage time $\langle n_{\text{FP}} \rangle$, as a function of resetting probability p_r . The red (blue) color intensity increases with threshold distance $N_r : 1 - 4$ (target's distances $x_T = 5, 8$). For each red color (fixed N_r), (blue) data is collapsed for two target's distances $x_T = 5, 8$.

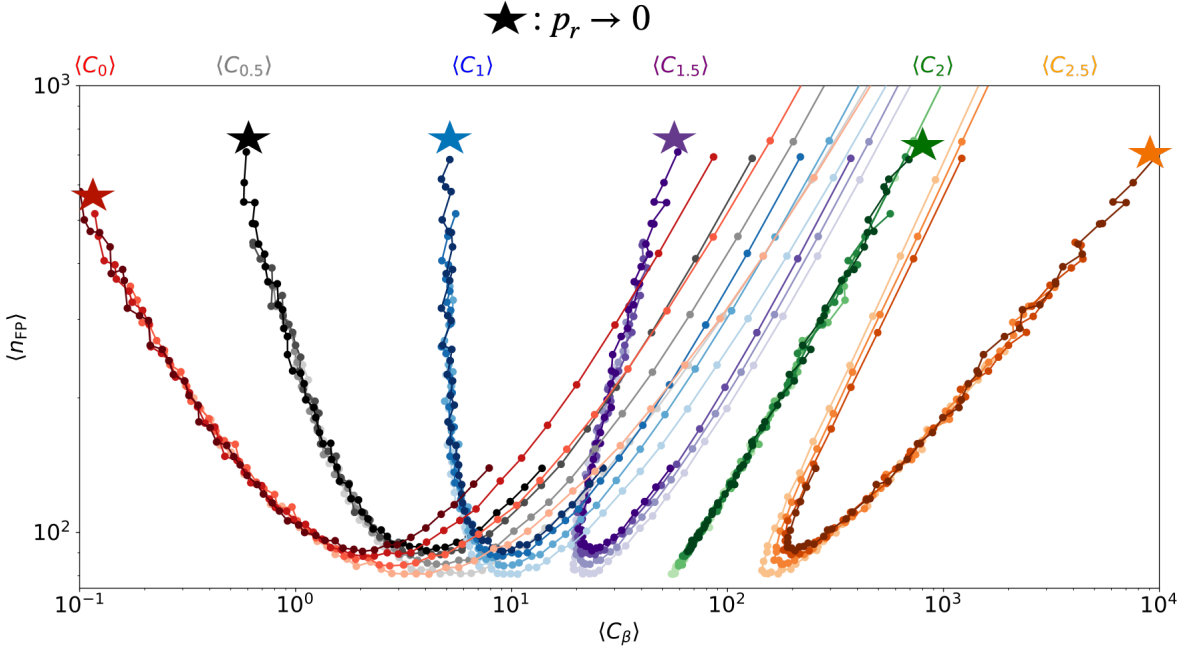


FIG. 8. Unbiased random walk ($p = q = 1/2$). Mean first passage time $\langle n_{\text{FP}} \rangle$ as a function of mean cost $\langle C_\beta \rangle$ (4) for target distance $x_T = 5$. The color intensity increases with threshold distance N_r (Fig. 3). Connecting lines are guide to the eye. Star indicates the direction of $p_r \rightarrow 0$ limit.

distance in Fig. 7(e-f). $\langle C_0 \rangle / \langle n_{\text{FP}} \rangle = p_r$ [Eq. (B31)] for $N_r = 1$. This is expected because MFPT increases with the target distance so does the mean number of resets; this makes the ratio to be independent of x_T . For $\beta = 0 - 1.5$, mean cost per MFPT reduces with increasing N_r , and for $\beta = 2$, this ratio insensitive to the value of N_r , where this ratio increases with N_r for $\beta = 2.5$.

Figure 8 discuss the trade-off relation between the mean first passage time and the mean cost of resetting $\langle C_\beta \rangle$ for different exponents β . Each curve is parameterized by the resetting probability, p_r . In the limit of $p_r \rightarrow 0$, the behavior is independent of N_r . (Star symbol indicates the direction of $p_r \rightarrow 0$ limit.) For each exponent β and N_r , MFPT can be optimized with respect to the mean cost, and the former has a global minimum for $N_r = 1$ for all cases (see the lightest colored symbols). For $\beta < 2$, the cost to achieve a certain MFPT is lower for larger N_r , whereas the trends is opposite for $\beta > 2$ in the limit $p_r \rightarrow 1$.

IV. CONCLUSION

In this paper, we investigated the dynamic stochastic resetting protocol, whereby a system resets with probability p_r only when it jumps a given number of steps in a direction. We specifically studied the impact of this protocol on the first passage time of the 1D infinite lattice random walk. Additionally, we computed the cost (4) of stochastic resetting until the walker hits the target/absorbing boundary for the first time. Our analysis revealed that this dynamic protocol is effective (in contrary to traditional resetting) in finding the target in the limit of large resetting probability p_r . The protocol allows to optimize the cost of resetting, and this optimization depends on the nature of cost function.

This study opens several research avenues in the field of stochastic resetting. It would be interesting to extend the analysis for other cases when the space is either continuous or discrete and time is

continuous, including extension to higher dimensions. An interesting question for future investigations (but beyond the scope of this paper) would be to compare results of dSR with that of the periodic dynamical stochastic resetting, where the counter, σ , [Eq. (1)] resets with probability 1 whenever $|\sigma| = N_r$ and the walker resets to the resetting location with probability p_r .

ACKNOWLEDGMENTS

This study was supported by the Special Research Fund (BOF) of Hasselt University (BOF number: BOF24KV10). This research was enabled in part by support provided by BC DRI Group and the Digital Research Alliance of Canada (www.alliancecan.ca).

Appendix A: Probability distribution function for $N_r = 1$

In this section, we compute the probability distribution function of a random walker to be at position x in time n starting from initial position $x = x_0$ undergoing the tradition stochastic resetting mechanism with $N_r = 1$ (in the absence of absorbing boundary). In this case, after every spatial jump a reset check is made. Hence, with probability $0 \leq p_r \leq 1$, the random walker resets to position $x = x_0$; otherwise, the random walker hops to left or right according to the underlying dynamical model. To compute the probability distribution $P(x, n|x_0)$, we compute the contribution from different trajectories that depend on the number of resetting events

$$P(x, n|x_0) = \sum_{m=0}^{\infty} \psi_m(x, n|x_0) , \quad (\text{A1})$$

with $\psi_m(x, n|x_0)$ the contribution from all trajectories for which exactly m resets occur.

For trajectories without a single reset, the contribution to the probability distribution is

$$\psi_0(x, n|x_0) = (1 - p_r)^n P_{\text{NR}}(x, n|x_0) , \quad (\text{A2})$$

where $(1 - p_r)^n$ be the probability of not a single resetting event up to time n , and during that duration the walker freely propagates with the probability distribution $P_{\text{NR}}(x, n|x_0)$. For one resetting event, the contribution is

$$\psi_1(x, n|x_0) = \sum_{m=1}^n \underbrace{(1 - p_r)^{m-1} p_r}_{I_1} \underbrace{(1 - p_r)^{n-m} P_{\text{NR}}(x, n - m|x_0)}_{I_2} , \quad (\text{A3})$$

where I_1 is the term corresponding to the random walker not resetting the first $m - 1$ times, and then, system resets to x_0 at m -th time. I_2 corresponds to those trajectories which have not reset in the remaining $n - m$ time. Therefore, we write Eq. (A3) using Eq. (A2):

$$\psi_1(x, n|x_0) = p_r \sum_{m=1}^n (1 - p_r)^{m-1} \psi_0(x, n - m|x_0) . \quad (\text{A4})$$

Similarly, we can write the contribution to the probability distribution for \mathcal{N}_r resets by generalizing Eq (A4):

$$\psi_{\mathcal{N}_r}(x, n|x_0) = p_r \sum_{m=1}^n (1 - p_r)^{m-1} \psi_{\mathcal{N}_r-1}(x, n - m|x_0) . \quad (\text{A5})$$

The above equation corresponds to the first-renewal mechanism. To compute the probability distribution $P(x, n|x_0)$, we z -transform Eq. (A5), and it gives

$$\tilde{\psi}_{\mathcal{N}_r}(x, z|x_0) = \frac{p_r}{1-p_r} \sum_{n=0}^{\infty} z^n \left[\sum_{m=0}^n (1-p_r)^m - \delta_{m,0} \right] \psi_{\mathcal{N}_r-1}(x, n-m|x_0), \quad (\text{A6})$$

$$= \frac{p_r}{1-p_r} \left[\sum_{m=0}^{\infty} \sum_{n=m}^{\infty} z^n (1-p_r)^m \psi_{\mathcal{N}_r-1}(x, n-m|x_0) - \tilde{\psi}_{\mathcal{N}_r-1}(x, z|x_0) \right], \quad (\text{A7})$$

$$= \frac{z p_r}{1-z(1-p_r)} \tilde{\psi}_{\mathcal{N}_r-1}(x, z|x_0). \quad (\text{A8})$$

The above equation (A8) is a recursive relation, which can be simplified as

$$\tilde{\psi}_{\mathcal{N}_r}(x, z|x_0) = \left[\frac{z p_r}{1-z(1-p_r)} \right]^{\mathcal{N}_r} \tilde{\psi}_0(x, z|x_0). \quad (\text{A9})$$

Then, the full propagator in z -space can be written by summing over \mathcal{N}_r from 0 to ∞ , and this gives

$$\tilde{P}(x, z|x_0) = \frac{1-z(1-p_r)}{1-z} \psi_0(x, z|x_0), \quad (\text{A10})$$

$$= \frac{1-z(1-p_r)}{1-z} \tilde{P}_{\text{NR}}(x, z(1-p_r)|x_0). \quad (\text{A11})$$

The above equation connects the propagator of the random walk under resetting $\tilde{P}(x, z|x_0)$ with that of in the absence of resetting $\tilde{P}_{\text{NR}}(x, z|x_0)$ [see Eq. (A13)]. Then, the stationary state distribution is obtained as

$$P^{\text{ss}}(x) \equiv \lim_{z \rightarrow 1} [(1-z)\tilde{P}(x, z|x_0)] = p_r \tilde{P}_{\text{NR}}(x, 1-p_r|x_0), \quad (\text{A12})$$

where

$$\tilde{P}_{\text{NR}}(x, z|x_0) \equiv \frac{1}{\sqrt{1-4pqz^2}} \left[\frac{1-\sqrt{1-4pqz^2}}{2zq} \right]^{|x-x_0|} \quad (\text{A13})$$

the z -transformed probability distribution function of the random walker starting from x_0 and reaching at x in the absence of both resetting mechanism and absorbing boundary $\tilde{P}_{\text{NR}}(x, z|x_0)$ is (see Eq. (1.3.11) in [51]). See Ref. [52] for a derivation of the stationary distribution of a random walk under stochastic resetting using the last renewal method and a different form of reset-free distribution $\tilde{P}_{\text{NR}}(x, z|x_0)$ [53].

Appendix B: Moment generating function of first passage time and cost for $N_r = 1$

In the following, we compute the moment generating function of the cost, C_β (4):

$$\Phi(k, n_{\text{FP}}|x_0) \equiv \langle e^{ikC_\beta} \rangle = \sum_{\mathcal{N}_r=0}^{\infty} \Psi_{\mathcal{N}_r}(k, n_{\text{FP}}|x_0), \quad (\text{B1})$$

where \mathcal{N}_r is the number of resets until the random walker (performing traditional stochastic resetting, i.e., $N_r = 1$) hits the target for the first time, and the angular brackets indicate the averaging over ensemble of these trajectories. We perform the calculation by counting the contributions of each random walker's trajectory starting from $x = x_0$, stochastically resetting to $x = x_0$, and hitting the target at $x = x_T$ for the first time at n_{FP} . We calculate the contributions of such trajectories for a given number of resets. (For convenience, henceforth we drop the subscript 'FP' from n_{FP} .)

- The contribution of trajectories of not having a single reset event (i.e., the random walker hits the target before the first resetting event) to the cost's (4) characteristic function is

$$\Psi_0(k, n|x_0) = (1 - p_r)^n F_{\text{NR}}(n|x_0) , \quad (\text{B2})$$

where the first and second terms, respectively, on the right-hand side (rhs) are the probability of not resetting up to the first passage time n and the first passage distribution of a reset-free random walker starting from $x = x_0$ and hitting the target $x = x_T$ for the first time. Notice that for this case, the cost C_β is zero.

- For one resetting event, we have

$$\Psi_1(k, n|x_0) = p_r \sum_{m=1}^n (1 - p_r)^{m-1} \phi_{\text{NR}}(k, m-1|x_0) (1 - p_r)^{n-m} F_{\text{NR}}(n-m|x_0) , \quad (\text{B3})$$

$$= p_r \sum_{m=1}^n (1 - p_r)^{m-1} \phi_{\text{NR}}(k, m-1|x_0) \Psi_0(k, n-m|x_0) , \quad (\text{B4})$$

where we used $F_{\text{NR}}(0|x_0) = 0$ in Eq. (B3), Eq. (B2) in Eq. (B4), and defined the reset-free (indicated by subscript 'NR') moment generating function of the cost:

$$\phi_{\text{NR}}(k, m|x_0) \equiv \sum_{x=-\infty}^{x_T} e^{ik|x-x_0|^\beta} P_{\text{NR}}^{\text{abs}}(x, n|x_0) , \quad (\text{B5})$$

for the absorbing boundary at $x = x_T$ and the reset-free random walker's probability distribution, $P_{\text{NR}}^{\text{abs}}(x, n|x_0)$, to be at x starting from $x = x_0$ in the presence of absorbing boundary at $x = x_T$. Notice that for $k = 0$, rhs of Eq. (B5) is the reset-free random walker's survival probability, $S_{\text{NR}}(n|x_0)$.

- Since the process renews after each resetting event, we generalize the contribution for \mathcal{N}_R resets by looking at Eq. (B4):

$$\Psi_{\mathcal{N}_r}(k, n|x_0) = p_r \sum_{m=1}^n (1 - p_r)^{m-1} \phi_{\text{NR}}(k, m-1|x_0) \Psi_{\mathcal{N}_r-1}(k, n-m|x_0) . \quad (\text{B6})$$

In order to proceed, we z -transform the above equation (B6):

$$\tilde{\Psi}_{\mathcal{N}_r}(k, z|x_0) = p_r \sum_{n=0}^{\infty} z^n \sum_{m=0}^{n-1} (1 - p_r)^m \phi_{\text{NR}}(k, m|x_0) \Psi_{\mathcal{N}_r-1}(k, n-m-1|x_0) \quad (\text{B7})$$

$$= zp_r \sum_{m=0}^{\infty} z^m (1 - p_r)^m \phi_{\text{NR}}(k, m|x_0) \sum_{n=1}^{\infty} z^{n-1} \Psi_{\mathcal{N}_r-1}(k, n-1|x_0) \quad (\text{B8})$$

$$= zp_r \tilde{\phi}_{\text{NR}}(k, z(1 - p_r)|x_0) \tilde{\Psi}_{\mathcal{N}_r-1}(k, z|x_0) \quad (\text{B9})$$

$$= [zp_r \tilde{\phi}_{\text{NR}}(k, z(1 - p_r)|x_0)]^{\mathcal{N}_r} \tilde{\Psi}_0(k, z|x_0) . \quad (\text{B10})$$

Summing over all reset numbers \mathcal{N}_r from 0 to ∞ , we get

$$\tilde{\Phi}(k, z|x_0) = \frac{\tilde{F}_{\text{NR}}(z(1 - p_r)|x_0)}{1 - zp_r \tilde{\phi}_{\text{NR}}(k, z(1 - p_r)|x_0)} , \quad (\text{B11})$$

where we used the z -transformed $\tilde{\Psi}_0(k, z|x_0)$ [see Eq. (B2)].

1. Moment generating function for first passage time

For Fourier variable $k = 0$, the above Eq. (B11) gives relation between the moment generating function of the first passage time in the presence of resetting with that of in the absence of resetting:

$$\tilde{F}(z|x_0) = \frac{\tilde{F}_{\text{NR}}(z(1-p_r)|x_0)}{1 - zp_r\tilde{S}_{\text{NR}}(z(1-p_r)|x_0)} . \quad (\text{B12})$$

We can write the above relation (B12) in terms of survival probability by noticing the relation between the first passage distribution at time n and the survival probability:

$$F(n|x_0) = S(n-1|x_0) - S(n|x_0) . \quad (\text{B13})$$

The z -transform of this gives

$$\tilde{F}(z|x_0) = (z-1)\tilde{S}(z|x_0) + 1 , \quad (\text{B14})$$

which ensures normalization for $z = 1$, as expected.

Substituting Eq. (B14) on the lhs of Eq. (B12) and rearranging terms, we get the z -transformed survival probability in the presence of resetting:

$$\tilde{S}(z|x_0) = \frac{1}{z-1} \frac{\tilde{F}_{\text{NR}}(z(1-p_r)) + zp_r\tilde{S}_{\text{NR}}(z(1-p_r)) - 1}{1 - zp_r\tilde{S}_{\text{NR}}(z(1-p_r))} . \quad (\text{B15})$$

Notice the relation (B14) also holds for reset-free dynamics. Therefore, replacing $z \rightarrow z(1-p_r)$, we get

$$\tilde{F}_{\text{NR}}(z(1-p_r)|x_0) = (z(1-p_r) - 1)\tilde{S}_{\text{NR}}(z(1-p_r)|x_0) + 1 . \quad (\text{B16})$$

Substituting Eq. (B16) on the rhs of Eq. (B15), we get

$$\tilde{S}(z|x_0) = \frac{\tilde{S}_{\text{NR}}(z(1-p_r))}{1 - zp_r\tilde{S}_{\text{NR}}(z(1-p_r))} . \quad (\text{B17})$$

This equation (already derived in Ref. [52, 54]) provides the connection between survival probabilities of reset and reset-free dynamics. In the following, we discuss the moments of the first passage time.

Differentiating both sides of Eq. (B14) with respect to z , we get

$$\tilde{F}'(z|x_0) = (z-1)\tilde{S}'(z|x_0) + \tilde{S}(z|x_0) , \quad (\text{B18})$$

which for $z = 1$ becomes

$$\tilde{F}'(1) = \tilde{S}(1) . \quad (\text{B19})$$

Here lhs is the mean first passage time $\langle n_{\text{FP}} \rangle$; therefore, $\langle n_{\text{FP}} \rangle$ can be evaluated from the survival probability (B17) by substituting $z = 1$ on both sides:

$$\langle n_{\text{FP}} \rangle = \frac{\tilde{S}_{\text{NR}}(1-p_r)}{1 - p_r\tilde{S}_{\text{NR}}(1-p_r)} . \quad (\text{B20})$$

Similarly, taking one more derivative of Eq. (B18) with respect to z and then setting $z = 1$, we get

$$\tilde{F}''(1) = 2\tilde{S}'(1) , \quad (\text{B21})$$

where the lhs is $\langle n_{\text{FP}}^2 \rangle - \langle n_{\text{FP}} \rangle$. Then, using the mean first passage time (B20), we can compute the second moment of first passage time.

The calculation shown in this section are valid for any dimensions. In the following, we specialize for the case of one dimensional random walker. To compute the mean first passage time (B20), we recognize the relation between the survival probability and the probability distribution function of the random walker (see Eq. (1.2.2) in [51]):

$$\tilde{S}_{\text{NR}}(z|x_0) = \frac{1}{1-z} \left[1 - \frac{\tilde{P}_{\text{NR}}(x, z|x_0)}{\tilde{P}_{\text{NR}}(x, z|x)} \right]. \quad (\text{B22})$$

where $\tilde{P}_{\text{NR}}(x, z|x)$ is given in Eq (A13). We emphasize that the relation (B22) holds even for the case of resetting dynamics.

Substituting Eq. (B22) by setting $z = 1 - p_r$ in Eq. (B20) gives the mean first passage time:

$$\langle n_{\text{FP}} \rangle = \frac{2^{|x_T - x_0|} T_1^{-1} - 1}{p_r}, \quad (\text{B23})$$

for

$$T_1 \equiv \left[\frac{1 - T_2}{q(1 - p_r)} \right]^{|x_T - x_0|}, \quad (\text{B24})$$

$$T_2 \equiv \sqrt{1 - 4pq(1 - p_r)^2}. \quad (\text{B25})$$

Here, x_T and x_0 , respectively, target location and initial position of the random walker. Similarly, we can compute the variance of the first passage time using Eqs. (B21) and (B23):

$$\begin{aligned} \langle [n_{\text{FP}} - \langle n_{\text{FP}} \rangle]^2 \rangle &= \frac{T_2(4^{|x_T - x_0|} + p_r T_1^2) - 2^{|x_T - x_0|} T_1 [T_2 + p_r(T_2 + |x_T - x_0|)]}{p_r^2 T_1^2 T_2} + \\ &+ \langle n_{\text{FP}} \rangle - \langle n_{\text{FP}} \rangle^2 \end{aligned} \quad (\text{B26})$$

$$= \frac{4^{|x_T - x_0|} T_2 - 2^{|x_T - x_0|} T_1 T_2 - 2^{|x_T - x_0|} p_r T_1 |x_T - x_0|}{p_r^2 T_1^2 T_2} - \langle n_{\text{FP}} \rangle^2. \quad (\text{B27})$$

2. Moment generating function of cost

Substituting $z = 1$ in Eq. (B11) gives the moment generating function of the cost (4) averaged over all first passage times:

$$\tilde{\Phi}(k, 1|x_0) = \frac{\tilde{F}_{\text{NR}}(1 - p_r|x_0)}{1 - p_r \tilde{\phi}_{\text{NR}}(k, 1 - p_r|x_0)}. \quad (\text{B28})$$

Differentiating with respect to ik and setting $k = 0$, we find the mean cost of resetting:

$$\langle C_\beta \rangle = p_r \frac{\tilde{F}_{\text{NR}}(1 - p_r|x_0)}{[1 - p_r \tilde{S}_{\text{NR}}(1 - p_r|x_0)]^2} \sum_{x=-\infty}^{x=x_T} |x|^\beta \tilde{P}_{\text{NR}}^{\text{abs}}(x, 1 - p_r|x_0) \quad (\text{B29})$$

$$= p_r \langle n_{\text{FP}} \rangle \frac{\sum_{x=-\infty}^{x=x_T} |x|^\beta \tilde{P}_0^{\text{abs}}(x, 1 - p_r|x_0)}{S_{\text{NR}}(1 - p_r|x_0)}, \quad (\text{B30})$$

where $\tilde{P}^{\text{abs}}(x, z|x_0)$ is the z -transformed probability distribution of a random walker to be at x starting from $x = x_0$ in the presence of absorbing boundary at $x = x_T$. Clearly, for $\beta = 0$, the mean cost (which is the average number of resets)

$$\langle C_0 \rangle = p_r \langle n_{\text{FP}} \rangle, \quad (\text{B31})$$

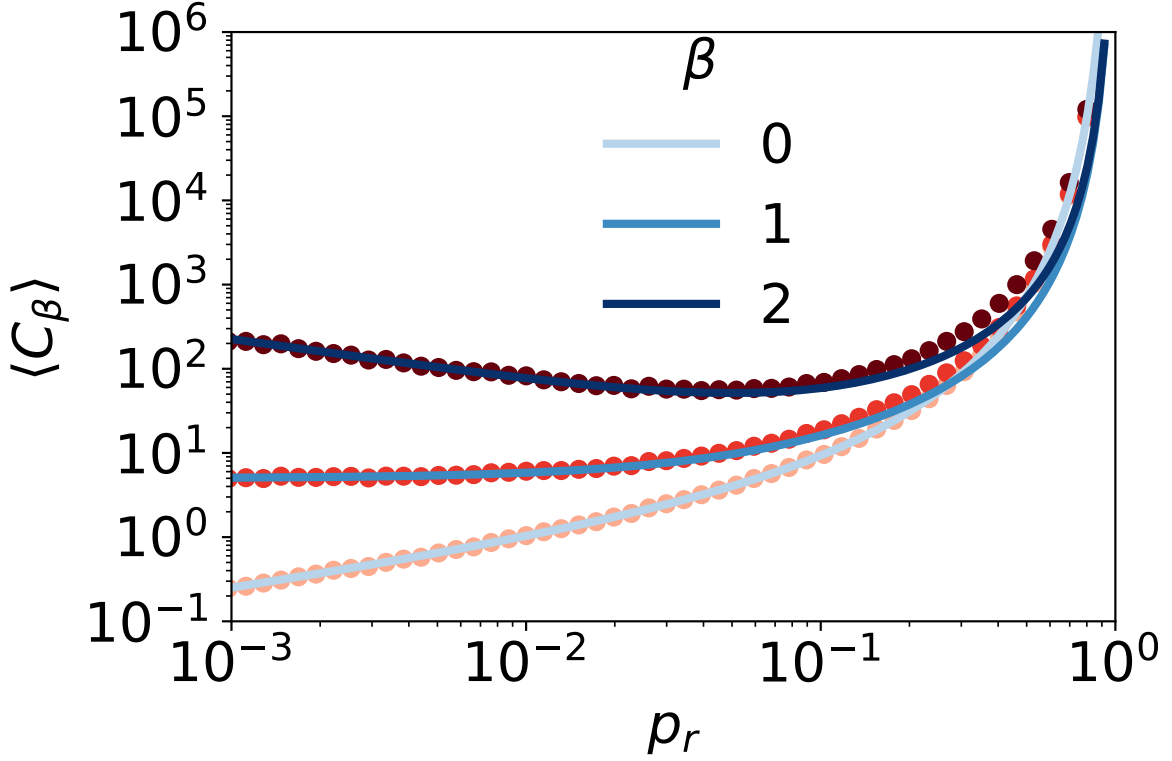


FIG. B1. Unbiased random walk ($p = q = 1/2$). Mean cost, $\langle C_\beta \rangle$ (4), as a function of resetting probability p_r . Symbols (red): Numerical simulation data. Curves (blue): Analytical prediction (B30) for $N_r = 1$. Here, the target is at $x_T = 5$. The color intensity increases with the exponent β .

as expected.

For a symmetric 1D random walk ($p = q$), $\tilde{P}_{\text{NR}}^{\text{abs}}(x, z)$ can be computed using the method of images:

$$\tilde{P}_{\text{NR}}^{\text{abs}}(x, z|x_0) \equiv \tilde{P}_{\text{NR}}(x, z|x_0) - \tilde{P}_{\text{NR}}(2x_T - x, z|x_0), \quad (\text{B32})$$

for $x_0 < x_T$. Using this relation (B32) we can compute the mean cost (B30).

Figure B1 displays the comparison of analytical result (B30) mean cost $\langle C_\beta \rangle$ with that of numerical simulation data for $N_r = 1$ and for three β values. We find small disagreement for large p_r value; this might be because of numerical evaluation of the summation in Eq. (B30).

Appendix C: Mean first passage time: $p_r \rightarrow 1$

Figure C1 discuss the mean first passage time for the random walker in the presence of dynamic resetting for $p_r = 1$. For $N_r = 1$ the MFPT diverges for for all $x_T \geq 1$, whereas MFPT diverges for $x_T \geq 2$ for $N_r = 2$. For other N_r , MFPT is finite. MFPT is optimized with respect to N_r , and it has minimum value for $N_r^* = x_T + 1$.

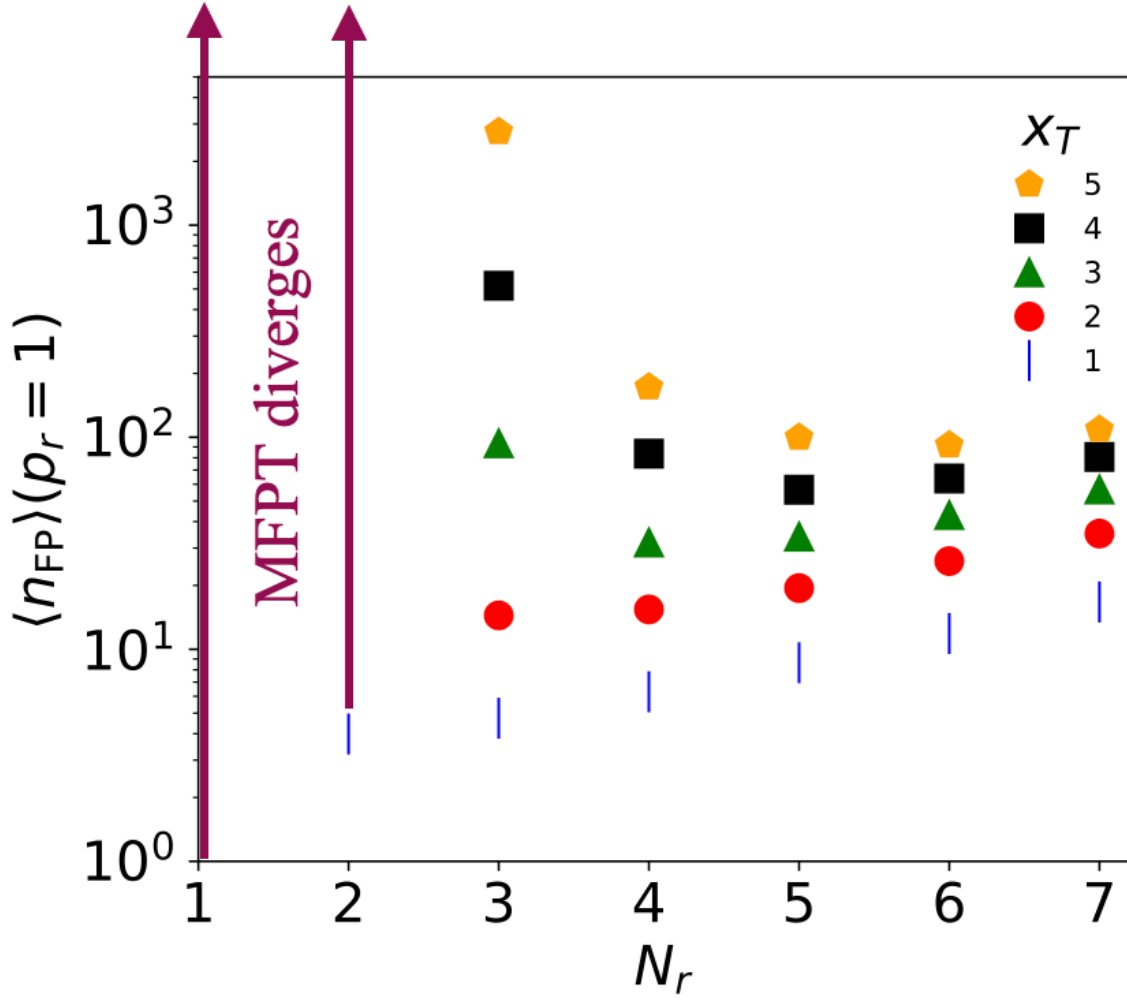


FIG. C1. Unbiased random walk ($p = q = 1/2$). Mean first passage time (MFPT) at resetting probability $p_r = 1$, as a function of threshold distance N_r for different target positions. For $N_r = 1$ the RW remains indefinitely at the reset position and the MFPT diverges as soon as $x_T \neq x_r$. For $N_r = 2$ the MFPT is finite for $x_T = 1$ and diverges otherwise. Symbols: Numerical simulation data.

Appendix D: Mean first passage time: Dynamic vs. window stochastic resetting

In this section, we compare the MFPT obtained from two different resetting schemes: 1) dynamic stochastic resetting (dSR), and 2) window stochastic resetting (wSR). In contrast to the dSR, wSR involves stochastically resetting the random walker to its initial location x_0 with probability p_r as soon as it hits either of the boundary of the window:

$$x_n = \begin{cases} x_{n-1} + 1 & \text{with probability } p \\ x_{n-1} - 1 & \text{with probability } 1 - p \\ x_0 & \text{with probability } p_r \text{ if } |x_n| \geq N_r. \end{cases} \quad (\text{D1})$$

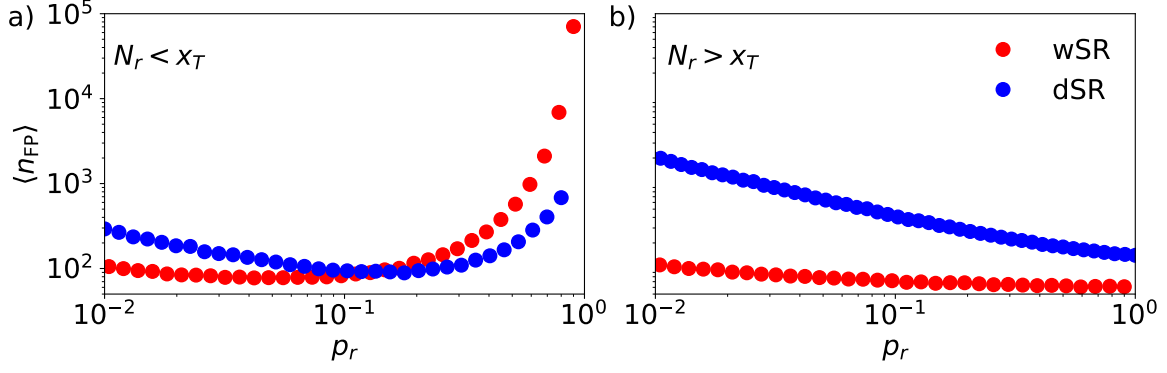


FIG. D1. Unbiased Random walk ($p = q = 1/2$). Blue: dynamic stochastic resetting (dSR) (1). Red: Window stochastic resetting (wSR) (D1). Threshold distance a) $N_r = 3$. b) $N_r = 7$. Target distance from resetting location $x_T = 5$.

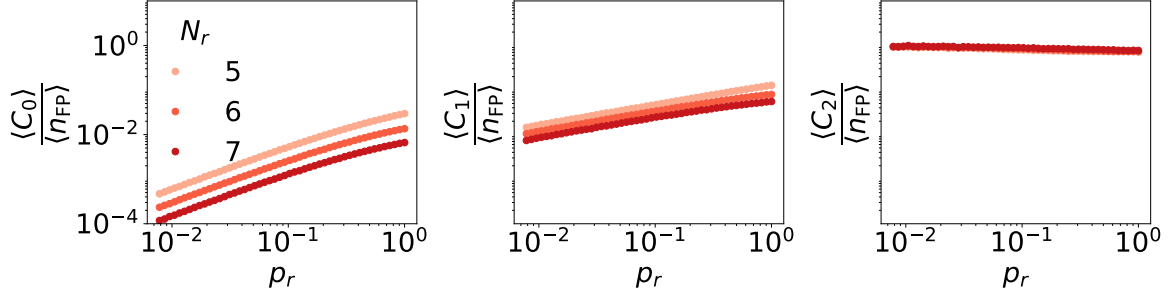


FIG. E1. Unbiased random walk ($p = q = 1/2$). Mean cost $\langle C_\beta \rangle$ (4) per mean first passage time as a function of resetting probability p_r . Symbols (red): Numerical simulation data. Here, the target is at $x_T = 5$. The color intensity increases with the exponent N_r .

Notice that wSR for a continuous space and continuous time is studied in Ref. [15]. We remind that N_r in dSR is the threshold of the total number of steps taken by the random walker in one direction. All resetting protocols, ie. dSR, wSR and tSR, are identical for $N_r = 1$.

Figure D1 shows the comparison of the MFPT of dSR with that of wSR for two different scenarios: (1) $N_r < x_T$, and (2) $N_r > x_T$. dSR has lower MFPT in scenario (1) for large p_r , whereas for scenario (2) wSR is better than dSR for all p_r .

Appendix E: Cost of resetting for $N_r \geq x_T$

Figure E1 discusses mean cost $\langle C_\beta \rangle$ per mean first passage time as a function of resetting probability p_r , for $N_r \geq x_T$. This ratio decreases as N_r increases for $\beta \leq 1$, and for $\beta = 2$, this is insensitive to N_r (as also seen in Fig. 7).

Appendix F: Method of simulations

In the following, we present the numerical simulation method to compute the first passage time and the cost C_β for 1D case. For convenience, we place the absorbing boundary x_T on the positive side of the origin, and reset the particle to the origin. We follow the dynamical rules as described in Eq. (1). To proceed, we initialize the position of the walker location ($x = x_0$), the counter ($\sigma = 0$), first passage time ($n_{\text{FP}} = 0$), and the cost ($C_\beta = 0$). Then, for each fixed x_T and N_r (threshold distance), we generate the following trajectory:

1. If $x \geq x_T$ the simulation stops [we go to step (6)]; otherwise, it continues as below.
2. With probability $p / 1 - p$, the random walker jumps to the right/left, and increase/decrease σ by one unit if it has a positive / negative value in the previous step; otherwise, we set it to $+1 / -1$.
3. Next if $|\sigma| \geq N_r$, we reset the random walker to the resetting location with probability p_r and update the cost by an amount of $|x - x_r|^\beta$, where x and x_r , respectively, are random walker's positions just before and after the reset.
4. We update the position x and advance the time by one unit.
5. We go back to step (1). This process iterates until the random walker hits the absorbing boundary (i.e., $x \rightarrow x_T$).
6. We record the first passage time n_{FP} and cost C_β .

We repeat the above algorithm for \mathcal{N}_R realizations to compute the statistics of first passage time and cost C_β .

REFERENCES

-
- [1] Hein A M, Carrara F, Brumley D R, Stocker R and Levin S A 2016 *Proceedings of the National Academy of Sciences* **113** 9413–9420 (*Preprint* <https://www.pnas.org/doi/pdf/10.1073/pnas.1606195113>) URL <https://www.pnas.org/doi/abs/10.1073/pnas.1606195113>
 - [2] Hein A M and McKinley S A 2012 *Proceedings of the National Academy of Sciences* **109** 12070–12074 (*Preprint* <https://www.pnas.org/doi/pdf/10.1073/pnas.1202686109>) URL <https://www.pnas.org/doi/abs/10.1073/pnas.1202686109>
 - [3] Berg O G, Winter R B and Von Hippel P H 1981 *Biochemistry* **20** 6929–6948
 - [4] Reuveni S, Urbakh M and Klafter J 2014 *Proceedings of the National Academy of Sciences* **111** 4391–4396 (*Preprint* <https://www.pnas.org/doi/pdf/10.1073/pnas.1318122111>) URL <https://www.pnas.org/doi/abs/10.1073/pnas.1318122111>
 - [5] Bell W 1991 *Searching behaviour*
 - [6] Bénichou O, Loverdo C, Moreau M and Voituriez R 2011 *Rev. Mod. Phys.* **83**(1) 81–129 URL <https://link.aps.org/doi/10.1103/RevModPhys.83.81>
 - [7] Bartumeus F and Catalan J 2009 *Journal of Physics A: Mathematical and Theoretical* **42** 434002 URL <https://dx.doi.org/10.1088/1751-8113/42/43/434002>
 - [8] Berg H C 2004 *E. coli in Motion* (Springer)
 - [9] Reingruber J and Holcman D 2011 *Phys. Rev. E* **84**(2) 020901 URL <https://link.aps.org/doi/10.1103/PhysRevE.84.020901>
 - [10] Wang F, Redding S, Finkelstein I J, Gorman J, Reichman D R and Greene E C 2013 *Nature Structural & Molecular Biology* **20** 174–181 ISSN 1545-9985 URL <https://doi.org/10.1038/nsmb.2472>

- [11] Luby M, Sinclair A and Zuckerman D 1993 *Information Processing Letters* **47** 173–180
- [12] Montanari A and Zecchina R 2002 *Physical review letters* **88** 178701
- [13] Evans M R and Majumdar S N 2011 *Physical review letters* **106** 160601
- [14] Evans M R, Majumdar S N and Schehr G 2020 *Journal of Physics A: Mathematical and Theoretical* **53** 193001
- [15] Evans M R and Majumdar S N 2011 *J. Phys. A Math. Theor.* **44** 435001 URL <https://doi.org/10.1088/1751-8113/44/43/435001>
- [16] Pal A, Kundu A and Evans M R 2016 *Journal of Physics A: Mathematical and Theoretical* **49** 225001
- [17] Shkilev V 2017 *Physical Review E* **96** 012126
- [18] Nagar A and Gupta S 2016 *Physical Review E* **93** 060102
- [19] Bonomo O L and Pal A 2021 *Phys. Rev. E* **103**(5) 052129 URL <https://link.aps.org/doi/10.1103/PhysRevE.103.052129>
- [20] Plata C A, Gupta D and Azaele S 2020 *Phys. Rev. E* **102**(5) 052116 URL <https://link.aps.org/doi/10.1103/PhysRevE.102.052116>
- [21] Bressloff P C 2020 *J. Phys. A Math. Theor.* **53** 355001 URL <https://doi.org/10.1088/1751-8121/ab9fb7>
- [22] Evans M R and Majumdar S N 2018 *Journal of Physics A: Mathematical and Theoretical* **52** 01LT01 URL <https://dx.doi.org/10.1088/1751-8121/aaf080>
- [23] García-Valladares G, Gupta D, Prados A and Plata C A 2024 *Physica Scripta* **99** 045234 URL <https://dx.doi.org/10.1088/1402-4896/ad317b>
- [24] Busiello D M, Gupta D and Maritan A 2021 *New Journal of Physics* **23** 103012 URL <https://doi.org/10.1088/1367-2630/ac2922>
- [25] Bao R and Hou Z 2022 Accelerating relaxation in markovian open quantum systems through quantum reset processes (*Preprint* 2212.11170)
- [26] Blumer O, Reuveni S and Hirshberg B 2024 *Nature Communications* **15** 240 ISSN 2041-1723 URL <https://doi.org/10.1038/s41467-023-44528-w>
- [27] Bae Y, Song Y and Jeong H 2024 Stochastic restarting to overcome overfitting in neural networks with noisy labels (*Preprint* 2406.00396)
- [28] Gupta D and Busiello D M 2020 *Phys. Rev. E* **102**(6) 062121 URL <https://link.aps.org/doi/10.1103/PhysRevE.102.062121>
- [29] Goerlich R and Roichman Y 2024 *arXiv preprint arXiv:2401.09958*
- [30] Goerlich R, Li M, Pires L B, Hervieux P A, Manfredi G and Genet C 2023 *arXiv preprint arXiv:2306.09503*
- [31] Bao R, Cao Z, Zheng J and Hou Z 2023 *Phys. Rev. Res.* **5**(4) 043066 URL <https://link.aps.org/doi/10.1103/PhysRevResearch.5.043066>
- [32] Santra I 2022 *Europhysics Letters* **137** 52001 URL <https://doi.org/10.1209/0295-5075/ac5e53>
- [33] Jolakoski P, Pal A, Sandev T, Kocarev L, Metzler R and Stojkoski V 2023 *Chaos, Solitons & Fractals* **175** 113921 ISSN 0960-0779 URL <https://www.sciencedirect.com/science/article/pii/S0960077923008226>
- [34] Cleuren B and Van den Broeck C 2002 *Phys. Rev. E* **65**(3) 030101 URL <https://link.aps.org/doi/10.1103/PhysRevE.65.030101>
- [35] Eichhorn R, Reimann P and Hänggi P 2002 *PHYSICAL REVIEW LETTERS* **88** ISSN 0031-9007
- [36] Cleuren B and Van den Broeck C 2003 *PHYSICAL REVIEW E* **67** ISSN 1539-3755
- [37] Ros A, Eichhorn R, Regtmeier J, Duong T, Reimann P and Anselmetti D 2005 *NATURE* **436** 928 ISSN 0028-0836
- [38] Machura L, Kostur M, Talkner P, Luczka J and Haenggi P 2007 *PHYSICAL REVIEW LETTERS* **98** ISSN 0031-9007
- [39] Sarracino A, Cecconi F, Puglisi A and Vulpiani A 2016 *PHYSICAL REVIEW LETTERS* **117** ISSN 0031-9007
- [40] Gupta D, Plata C A and Pal A 2020 *Phys. Rev. Lett.* **124**(11) 110608 URL <https://link.aps.org/doi/10.1103/PhysRevLett.124.110608>
- [41] Mori F, Olsen K S and Krishnamurthy S 2023 *Phys. Rev. Res.* **5**(2) 023103 URL <https://link.aps.org/doi/10.1103/PhysRevResearch.5.023103>
- [42] Olsen K S and Gupta D 2024 *Journal of Physics A: Mathematical and Theoretical* **57** 245001 URL <https://dx.doi.org/10.1088/1751-8121/ad4c2c>
- [43] Gupta D and Plata C A 2022 *New J. Phys. in press* <https://doi.org/10.1088/1367-2630/aca25e>
- [44] Olsen K S, Gupta D, Mori F and Krishnamurthy S 2023 *arXiv preprint arXiv:2310.11267*

- [45] Sunil J C, Blythe R A, Evans M R and Majumdar S N 2023 *Journal of Physics A: Mathematical and Theoretical* **56** 395001 URL <https://dx.doi.org/10.1088/1751-8121/acf3bb>
- [46] Pal P S, Pal A, Park H and Lee J S 2023 *Phys. Rev. E* **108**(4) 044117 URL <https://link.aps.org/doi/10.1103/PhysRevE.108.044117>
- [47] Busiello D M, Gupta D and Maritan A 2020 *Phys. Rev. Research* **2**(2) 023011 URL <https://link.aps.org/doi/10.1103/PhysRevResearch.2.023011>
- [48] Fuchs J, Goldt S and Seifert U 2016 *EPL (Europhysics Letters)* **113** 60009
- [49] Pal A, Reuveni S and Rahav S 2021 *Phys. Rev. Research* **3**(1) 013273 URL <https://link.aps.org/doi/10.1103/PhysRevResearch.3.013273>
- [50] Pal A and Reuveni S 2017 *Phys. Rev. Lett.* **118**(3) 030603 URL <https://link.aps.org/doi/10.1103/PhysRevLett.118.030603>
- [51] Redner S 2001 *A Guide to First-Passage Processes* (Cambridge University Press)
- [52] Das D and Giuggioli L 2022 *Journal of Physics A: Mathematical and Theoretical* **55** 424004 URL <https://dx.doi.org/10.1088/1751-8121/ac9765>
- [53] Sarvaharman S and Giuggioli L 2020 *Phys. Rev. E* **102**(6) 062124 URL <https://link.aps.org/doi/10.1103/PhysRevE.102.062124>
- [54] Kusmierz L, Majumdar S N, Sabhapandit S and Schehr G 2014 *Physical review letters* **113** 220602